LETTERS
PUBLISHED ONLINE: 19 JANUARY 2015 | DOI: 10.1038/NGEO2345
nature geoscience

Circulation response to warming shaped by radiative changes of clouds and water vapour

Aiko Voigt[1]* and Tiffany A. Shaw[1,2,3]

The atmospheric circulation controls how global climate change will be expressed regionally. Substantial circulation changes are expected under global warming, including a narrowing of the intertropical convergence zone[1,2], a slow down and poleward expansion of the tropical circulation[3,4], and a poleward shift of mid-latitude stormtracks and jets[5,6]. Yet, climate model projections of the circulation response to climate change remain uncertain[7]. Here we present simulations with two different aquaplanet climate models and analyse these simulations using the cloud and water-vapour locking method. We find that radiative changes of clouds and water vapour are key to the regional response of precipitation and circulation to global warming. Model disagreement in the response of key characteristics of the atmospheric circulation—the intertropical convergence zone, the strength of the Hadley circulation, and the trade winds—arises from disagreement between the models in radiative changes of tropical ice clouds and their coupling to the circulation. We find that cloud changes amplify a poleward shift of the extratropical jet, whereas water vapour changes oppose such a shift, but the degree of compensation is model-dependent. We conclude that radiative changes of clouds and water vapour are not only integral to the magnitude of future global-mean warming but also determine patterns of regional climate change.

Precipitation controls the availability of water. Because changes in precipitation have profound impacts on societies, economies and ecosystems, a key concern in climate science is the response of precipitation to global warming. Climate models robustly project an increase of global-mean precipitation at a rate of 1–3% per degree warming[3,7]. There is less consensus, however, on how the global-mean increase will be distributed regionally, and confidence in long-term projections of regional precipitation changes remains much lower than for temperature[8]. The model spread persists from previous model intercomparisons despite increased model complexity and spatial resolution and is as large in idealized aquaplanet configurations with prescribed zonally uniform sea-surface temperatures (SSTs) as in realistic configurations that include detailed representations of the land surface, orography and sea ice[9,10]. Aquaplanets highlight the models' basic responses and elucidate the processes that lead to non-robustness[10–12], suggesting that they are a stepping stone towards improved understanding of realistic model configurations and, ultimately, the real climate system.

Aquaplanet simulations were included in phase 5 of the Coupled Model Intercomparison Project (CMIP5; ref. 13). The reference simulation aquaControl prescribes the zonally uniform SSTs of the 'qobs' profile defined by ref. 11, and the perturbed simulation aqua4K mimics global warming through a uniform increase of SSTs by 4 K. Figure 1 shows the time-mean precipitation change between aquaControl and aqua4K simulated by two CMIP5 models, MPI-ESM (ref. 14) and IPSL-CM5A (ref. 15). The models are run in their low-resolution (LR) versions; however, we omit the suffix LR that is used in the CMIP5 model naming convention for simplicity. Although the models simulate the same increase in global-mean precipitation of 0.5 mm d^{-1}, they disagree on the magnitude, meridional pattern and sign of the precipitation response in the deep tropics (15° N to 15° S). MPI-ESM predicts a maximum increase at the equator and a decrease directly poleward thereof, that is, a contraction of the intertropical convergence zone (ITCZ). IPSL-CM5A, in contrast, shows a weak increase throughout the entire deep tropics, with maxima at the equator and at 10° N/S—that is, a widening of the ITCZ. The equatorial increase in IPSL-CM5A is a factor of seven smaller (1.3 mm d^{-1} versus 9.2 mm d^{-1}; Fig. 2a). The differences in the regional response are surprising given the simple forcing and motivate us to better understand the two models, which sample the spectrum of tropical precipitation responses found in the CMIP5 aquaplanet model ensemble[9,10].

To quantify and understand the role of radiative changes of clouds and water vapour in the precipitation response, we perform further simulations using the cloud and water-vapour locking method (Methods). The locking method decomposes the response of precipitation, or more generally any variable, into a contribution

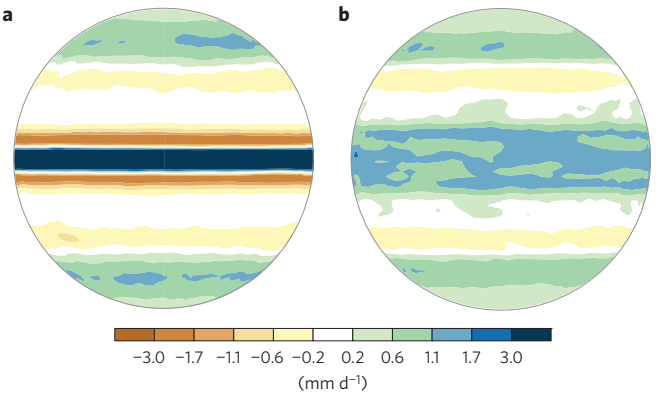

Figure 1 | Precipitation response in two CMIP5 aquaplanet models under a uniform 4 K surface warming. a, MPI-ESM model. **b**, IPSL-CM5A model. Time-mean values are shown.

[1]Lamont-Doherty Earth Observatory, Columbia University, 61 Route 9W, Palisades, New York 10964, USA. [2]Department of Earth and Environmental Sciences, Columbia University, New York, New York 10025, USA. [3]Department of Applied Physics and Applied Mathematics, Columbia University, New York, New York 10025, USA. *e-mail: aiko@ldeo.columbia.edu

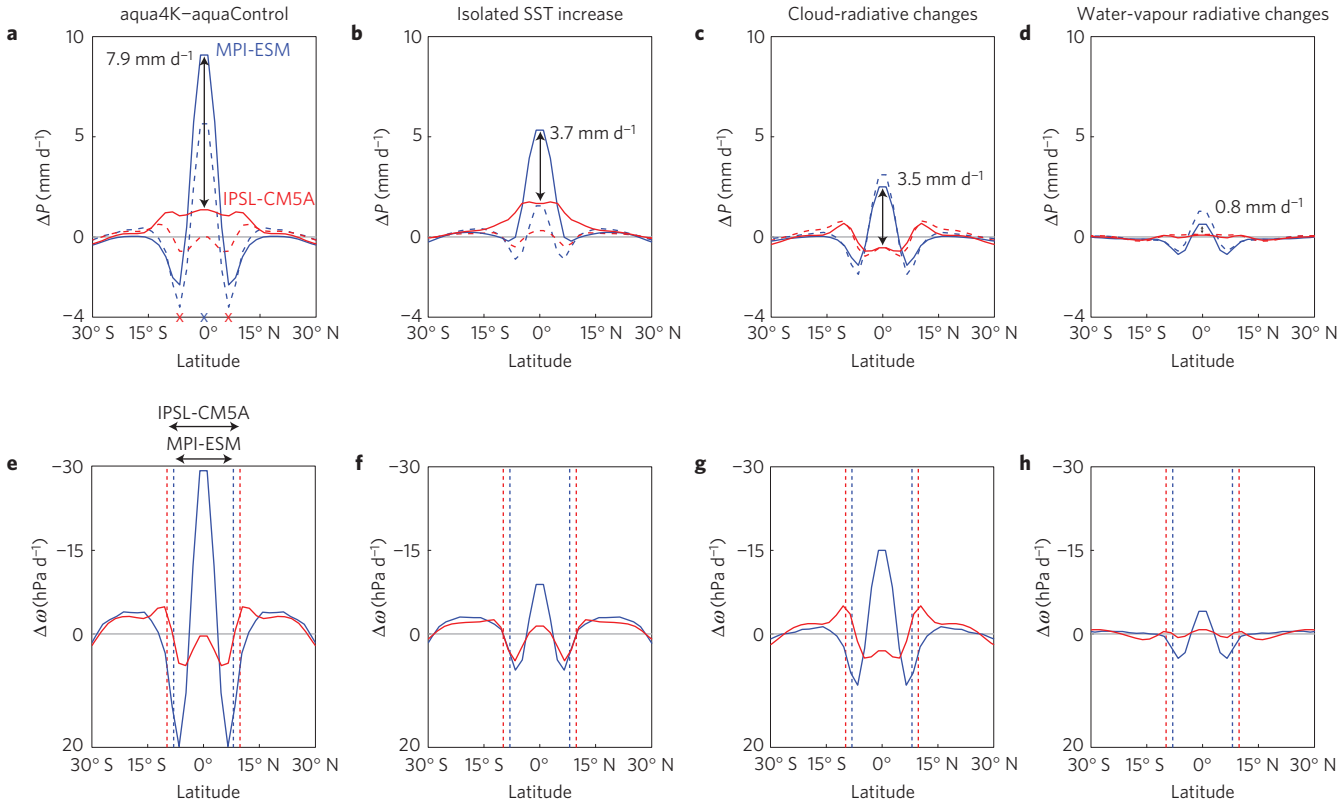

Figure 2 | Decomposition of tropical precipitation and vertical velocity response to global warming. a–d, Time- and zonal-mean precipitation response (**a**, crosses indicate the latitude of the precipitation maximum in aquaControl), contributions from the isolated SST increase (**b**), radiative changes of clouds (**c**) and radiative changes of water vapour (**d**). Dashed lines show the dynamic component of the precipitation response. Results according to the models MPI-ESM and IPSL-CMSA are shown in blue and red, respectively. **e–f**, Same for time- and zonal-mean pressure velocity averaged between 300 and 800 hPa. Dashed vertical lines give the latitude that separates the ascending from the descending Hadley circulation branch in aquaControl.

from the SST increase, assuming no radiative changes of clouds and water vapour, and contributions from the radiative changes of clouds and water vapour assuming no SST increase. The method helps to establish causality by breaking the interactions and feedbacks between radiation and the circulation. Compared to the deep-tropical precipitation response, the contribution of the isolated SST increase (no radiative changes of clouds and water vapour) shows a greater similarity between the models (Fig. 2b). Both models simulate maximum precipitation increase at the equator, and the model difference in the equatorial increase is reduced from 7.9 mm d^{-1} to 3.7 mm d^{-1}. Radiative changes of clouds are at least as important to the model disagreement as the isolated SST increase. They contribute as much to the model disagreement in the equatorial precipitation increase (3.5 mm d^{-1}, Fig. 2c) and are at the heart of the model disagreement in the meridional pattern of the response. Radiative changes of clouds increase equatorial and decrease off-equatorial precipitation in MPI-ESM, thereby contracting the ITCZ. They broaden the ITCZ in IPSL-CM5A by generating off-equatorial maxima.

One might suspect that the model disagreement in the precipitation response results from differences in the models' aquaControl precipitation, with MPI-ESM simulating a single ITCZ and IPSL-CM5A simulating a double ITCZ (crosses in Fig. 2a and Supplementary Fig. 1). According to the wet-get-wetter paradigm, these differences are accentuated under global warming owing to the increase in atmospheric water vapour content from the Clausius–Clapeyron relation and the associated thermodynamic component of the precipitation response[3]. However, the pattern of precipitation response is closely linked to the circulation response (Fig. 2a and e) and indeed arises from the dynamic component[16,17] (Fig. 2 and Supplementary Fig. 2). As a result both models do not simply follow the wet-get-wetter paradigm, which implies that understanding the disagreement in the pattern of precipitation response to the 4 K SST increase requires an understanding of the disagreement in the circulation response. This is especially important for the precipitation response to radiative changes of clouds, which results entirely from circulation changes (Fig. 2c).

The deep-tropical circulation responds very differently in the two models, consistent with the dynamic precipitation component (Fig. 2e). The response to the isolated SST increase, however, is much more similar (Fig. 2f). Indeed, both models respond to the isolated SST increase by weakening downward motion in the descending branch of the Hadley circulation, consistent with increased static stability (see below) and weak horizontal temperature gradients, and by expanding the Hadley circulation (Supplementary Table 1). In MPI-ESM the expansion is so strong that weaker downward motion does not translate into a weaker total mass flux, allowing the strength of the Hadley circulation to remain unchanged in response to the isolated SST increase. Radiative changes of clouds are the dominant source of disagreement in the circulation response (Fig. 2g and Supplementary Table 1). In MPI-ESM radiative changes of clouds produce anomalous upward motion close to the equator and contract the ascending branch of the Hadley circulation and the ITCZ. In IPSL-CM5A, in contrast, they widen the ascending branch of the Hadley circulation and the ITCZ. Radiative changes of clouds accelerate the Hadley circulation in MPI-ESM, leading to an overall stronger circulation with global warming. This is in sharp contrast to the weakening simulated by IPSL-CM5A as well as all other CMIP5 aquaplanet models[10].

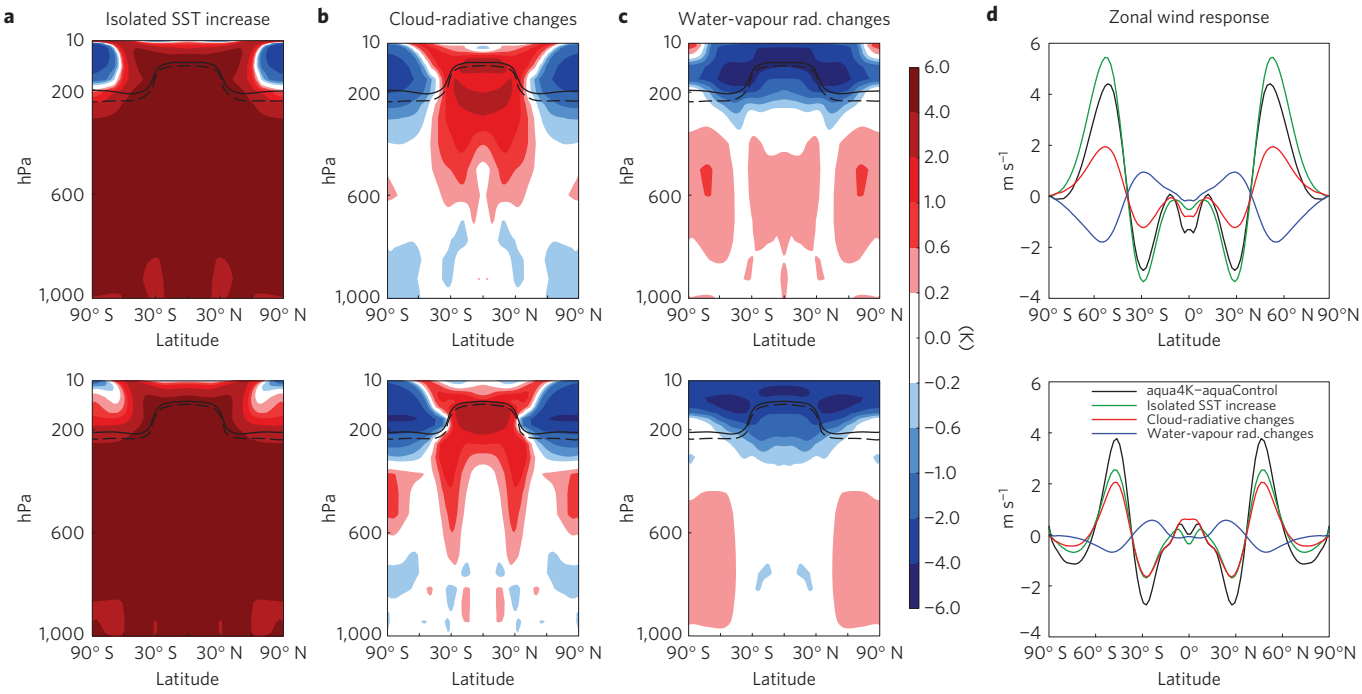

Figure 3 | Impact of radiative changes of clouds and water vapour on the atmospheric temperature and zonal wind response to global warming in MPI-ESM (top) and IPSL-CM5A (bottom). a–c, Time- and zonal-mean contributions of the isolated SST increase (**a**), and radiative changes of clouds (**b**) and water vapour (**c**) to the temperature response. The dashed and solid lines mark the tropopause of the aquaControl and aqua4K simulations, respectively. **d**, Time- and zonal-mean response of the 925 hPa zonal wind (black line) and its decomposition by the locking method (coloured lines).

In the deep tropics the radiative changes of clouds are dominated by changes in high-level tropical ice clouds. When imposed in the locked simulations, the changes in ice clouds heat the atmosphere in both models. This heating must be balanced by adiabatic cooling from upward motion and is key to the different circulation responses in the two models (Supplementary Fig. 3). The models, however, disagree in the latitudinal position of the ice cloud changes—and thus the anomalous upward motion—for at least two reasons. First, ITCZ differences in aquaControl imply that the upward cloud shift[18]—and thus the radiative heating—occurs at different latitudes. This source of disagreement would be eliminated if the models simulated the same ITCZ location in aquaControl. Second, tropical ice clouds undergo model-dependent meridional displacements: they contract towards the equator in MPI-ESM but extend further poleward in IPSL-CM5A (Supplementary Fig. 4). The full magnitude of the ice cloud displacements is realized only when clouds are allowed to affect the circulation via radiative heating, suggesting a positive feedback between cloud ice and upward motion. The isolated SST increase contributes a comparably small fraction to the cloud ice displacement. Despite being small, these cloud ice changes might seed the feedback and determine the direction of the ITCZ response. As they are not obviously related to changes in upward motion they may result from microphysical changes or cloud ice transport by the meridional flow that could be affected by eddy-momentum fluxes[19]. Disentangling the processes behind the cloud ice displacements is an important and challenging task for future studies, in particular because the CMIP5 aquaplanet ensemble shows no systematic relation between the location of the ITCZ in aquaControl and its response (Supplementary Fig. 5).

Poleward of 15° N/S the model responses are more robust. Nevertheless, radiative changes of clouds and water vapour still affect the large-scale circulation poleward of 15° N/S by generating spatially varying temperature patterns that modify the temperature response to the isolated SST increase (Fig. 3). Throughout the tropics, radiative changes of clouds increase the dry vertical stability by longwave-induced warming of the upper troposphere and lower stratosphere (UTLS), with some compensation from water vapour changes. In the extratropics, radiative changes of water vapour warm the troposphere but cool the stratosphere, and cloud changes warm the middle troposphere and cool the UTLS. Although each component of the temperature response potentially affects the circulation, tropical UTLS temperatures probably play a key role. By stabilizing the tropical atmosphere, radiative changes of clouds contribute to the expansion of the tropics (Supplementary Table 1) as they shift the latitude where the subtropical jet becomes unstable poleward[20,21]. Radiative changes of water vapour contract the tropics by destabilizing the tropical atmosphere.

The opposite impacts of clouds and water vapour on the width of the Hadley circulation suggest different impacts on the extratropical circulation. Figure 3 illustrates the response of the easterly trade winds and the westerly extratropical jet stream. Near the equator, radiative changes of clouds dominate the response of the trade winds, which intensify in MPI-ESM but weaken in IPSL-CM5A, reflecting the model disagreement in the response of the Hadley circulation strength. In the subtropics and extratropics, where moist convection is less important, there is more agreement in the response. Both models simulate a poleward shift of the extratropical jet in response to global warming, consistent with the predictions from coupled atmosphere–ocean models[5,6]. Consistent with their impact on the width of the tropics and because the jet and the subtropical edge of the Hadley circulation move in tandem in the simulations, radiative changes of clouds and water vapour produce opposite shifts of the extratropical jet. Radiative changes of clouds cause a poleward jet shift and determine around 40% of the maximum zonal wind response. In contrast, radiative changes of water vapour cause an equatorward jet shift. The jet shifts in response to radiative changes of cloud and water vapour almost completely cancel each other in MPI-ESM, but not in IPSL-CM5A, so that the net impact of radiative changes of clouds and water

vapour is close to zero in MPI-ESM but important in IPSL-CM5A. The model-dependent degree of compensation appears to be related to the model-dependent tropical UTLS (between 20° N/S and 70–150 hPa) temperature response to radiative changes of clouds and water vapour. In both models cloud changes warm the tropical UTLS by 1.5 K, although the water-vapour-induced cooling is larger in MPI-ESM (1.3 K versus 0.5 K in IPSL-CM5A). Future studies are needed to assess to what extent this model-dependent compensation accounts for the model spread in the magnitude of the poleward jet shift reported in realistic coupled ocean–atmosphere CMIP5 simulations[6].

Radiative changes of clouds and water vapour have long been known to be fundamental for the response of surface temperatures to global warming[22,23]. Here we show that they are equally important to the circulation response and that uncertainty in circulation changes is inherently linked to uncertainty in the behaviour of clouds and water vapour. This link, which is only beginning to be understood[24–26], suggests that advancing our understanding of how radiative changes of clouds and water vapour interact and couple with the circulation is required to improve projections of regional climate changes and to develop reliable climate adaptation strategies.

Methods

The cloud and water-vapour locking method decomposes the climate response into contributions from the isolated SST increase, the radiative changes of clouds, and the radiative changes of water vapour. The method thus quantifies how much of the response is generated by radiative changes of clouds or water vapour and how much of the model differences are caused by model differences in the radiative changes of clouds or water vapour. Variants of the method were originally used for radiative–temperature feedbacks[27,28] and have recently been applied to investigate the precipitation response to hemispherically asymmetric forcings[24,29,30]. Here we employ the method to examine the precipitation and circulation response to global warming. A strength of the method is that is allows us to study the effect of radiative changes of clouds and water vapour on the circulation response. For example, when the models are run with SST and water vapour taken from aquaControl but with clouds locked to aqua4K, the radiative changes of clouds from aquaControl to aqua4K introduce a radiative forcing that leads to a circulation response independent of changes in SSTs and the radiative properties of water vapour.

The method is used as follows. The instantaneous radiative properties of clouds and water vapour are stored at each call of the radiation transfer scheme in the aquaControl and aqua4K simulations (every 2 h in MPI-ESM, every hour in IPSL-CM5A). The aquaControl and aqua4K simulations are then repeated with the radiation being calculated with clouds and water vapour prescribed from, or 'locked' to, either aquaControl or aqua4K. The locking only affects the radiation calculation; convection and precipitation are not prescribed. This leads to the eight additional simulations: T1C1W1, T1C1W2, T1C2W1, T1C2W2, T2C1W1, T2C1W2, T2C2W1, T2C2W2. The numbers indicate whether sea-surface temperatures (T) of aquaControl ('simulation 1') or aqua4K ('simulation 2') are used, and whether the radiation transfer scheme uses clouds (C) and water vapour (W) from aquaControl or aqua4K. The locking decorrelates the radiative properties of clouds and water vapour from the atmospheric temperature and circulation—for example, the model can see the radiative heating tendencies of a deep convective cloud, whereas the actually simulated flow is that of cloud-free subsidence. The climatic effect of this decorrelation, however, is found to be small, so that the climate of T1C1W1 closely resembles that of aquaControl, and likewise for T2C2W2 and aqua4K (Supplementary Fig. 1). Thus, the response of a variable X, $\Delta X = X_{\mathrm{aqua4K}} - X_{\mathrm{aquaControl}}$, can be written as

$$\Delta X = X_{\mathrm{T2C2W2}} - X_{\mathrm{T1C1W1}} + R$$

R is generally much smaller than ΔX and $X_{\mathrm{T2C2W2}} - X_{\mathrm{T1C1W1}}$ (Supplementary Fig. 1), which is a prerequisite for the locking method to be meaningful. Following this decomposition, the contribution of the isolated SST increase to ΔX is given by

$$\Delta X_{\mathrm{SST}} = 0.5 \times [(X_{\mathrm{T2C1W1}} - X_{\mathrm{T1C1W1}}) + (X_{\mathrm{T2C2W2}} - X_{\mathrm{T1C2W2}})]$$

the contribution from radiative changes of clouds is given by

$$\Delta X_{\mathrm{clouds}} = 0.25 \times [(X_{\mathrm{T1C2W1}} - X_{\mathrm{T1C1W1}}) + (X_{\mathrm{T1C2W2}} - X_{\mathrm{T1C1W2}}) + (X_{\mathrm{T2C2W1}} - X_{\mathrm{T2C1W1}}) + (X_{\mathrm{T2C2W2}} - X_{\mathrm{T2C1W2}})]$$

and the contribution from radiative changes of water vapour is given by

$$\Delta X_{\mathrm{vapour}} = 0.25 \times [(X_{\mathrm{T1C1W2}} - X_{\mathrm{T1C1W1}}) + (X_{\mathrm{T1C2W2}} - X_{\mathrm{T1C2W1}}) + (X_{\mathrm{T2C1W2}} - X_{\mathrm{T2C1W1}}) + (X_{\mathrm{T2C2W2}} - X_{\mathrm{T2C2W1}})]$$

By construction the three contributions sum up to $(X_{\mathrm{T2C2W2}} - X_{\mathrm{T1C1W1}})$ so that

$$\Delta X = \Delta X_{\mathrm{SST}} + \Delta X_{\mathrm{clouds}} + \Delta X_{\mathrm{vapour}} + R$$

All simulations are run for 30 years, with the last 28 years being used in the analysis. We verified the implementation of the models on the computing cluster of the Lamont-Doherty Earth Observatory by comparing our aquaControl and aqua4K simulations to the CMIP5 archive. The simulation data are freely available from A.V. on request.

Received 10 July 2014; accepted 16 December 2014; published online 19 January 2015

References

1. Neelin, J. D., Chou, C. & Su, H. Tropical drought regions in global warming and El Niño teleconnections. *Geophys. Res. Lett.* **30,** 2275 (2003).
2. Huang, P., Xie, S-P., Hu, K., Huang, G. & Huang, R. Patterns of the seasonal response of tropical rainfall to global warming. *Nature Geosci.* **6,** 357–361 (2013).
3. Held, I. M. & Soden, B. J. Robust responses of the hydrological cycle to global warming. *J. Clim.* **19,** 5686–5699 (2006).
4. Lu, J., G. Vecchi, G. A. & Reichler, T. Expansion of the Hadley cell under global warming. *Geophys. Res. Lett.* **34,** L06805 (2007).
5. Yin, J. H. A consistent poleward shift of the storm tracks in simulations of 21st century climate. *Geophys. Res. Lett.* **32,** L18701 (2005).
6. Barnes, E. A. & Polvani, L. M. Response of the midlatitude jets and of their variability to increased greenhouse gases in CMIP5 models. *J. Clim.* **26,** 7117–7135 (2013).
7. Collins, M. *et al.* in *IPCC Climate Change 2013: The Physical Science Basis* (eds Stocker, T. *et al.*) Ch. 12, 1029–1136 (Cambridge Univ. Press, 2013).
8. Knutti, R. & Sedlacek, J. Robustness and uncertainties in the new CMIP5 climate model projections. *Nature Clim. Change* **3,** 369–373 (2013).
9. Stevens, B. & Bony, S. What are climate models missing? *Science* **340,** 1053–1054 (2013).
10. Medeiros, B., Stevens, B. & Bony, S. Using aquaplanets to understand the robust responses of comprehensive climate models to forcing. *Clim. Dynam.* 1–21 (2014).
11. Neale, R. B. & Hoskins, B. J. A standard test for AGCMs including their physical parametrizations: I: The proposal. *Atmos. Sci. Lett.* **1,** 101–107 (2000).
12. Blackburn, M. *et al.* The Aqua-Planet Experiment (APE): Control SST simulation. *J. Meteorol. Res. Jpn* **91A,** 17–56 (2013).
13. Taylor, K. E., Stouffer, R. J. & Meehl, G. A. An overview of CMIP5 and the experiment design. *Bull. Am. Meteorol. Soc.* **93,** 485–498 (2012).
14. Stevens, B. *et al.* Atmospheric component of the MPI-M Earth System Model: ECHAM6. *J. Adv. Model. Earth Syst.* **5,** 146–172 (2013).
15. Dufresne, J-L. *et al.* Climate change projections using the IPSL-CM5 Earth System Model: From CMIP3 to CMIP5. *Clim. Dynam.* **40,** 2123–2165 (2013).
16. Chou, C. & Neelin, J. D. Mechanisms of global warming impacts on regional tropical precipitation. *J. Clim.* **17,** 2688–2701 (2004).
17. Bony, S. *et al.* Robust direct effect of carbon dioxide on tropical circulation and regional precipitation. *Nature Geosci.* **6,** 447–451 (2013).
18. Hartmann, D. L. & Larson, K. An important constraint on tropical cloud–climate feedback. *Geophys. Res. Lett.* **29,** 1951 (2002).
19. Schneider, T. The general circulation of the atmosphere. *Annu. Rev. Earth Planet. Sci.* **34,** 655–688 (2006).
20. Held, I. M. *Woods Hole Oceanographic Institute Geophysical Fluid Dynamics Program* (Woods Hole Oceanogr. Institute, 2000); http://gfd.whoi.edu/proceedings/2000/PDFvol2000.html
21. Frierson, D. M. W., Lu, J. & Chen, G. Width of the Hadley cell in simple and comprehensive general circulation models. *Geophys. Res. Lett.* **34,** L18804 (2007).
22. Held, I. & Soden, B. Water vapor feedback and global warming. *Annu. Rev. Energy Environ.* **25,** 441–475 (2000).
23. Bony, S. & Dufresne, J-L. Marine boundary layer clouds at the heart of tropical cloud feedback uncertainties in climate models. *Geophys. Res. Lett.* **32,** L20806 (2005).
24. Voigt, A., Bony, S., Dufresne, J-L. & Stevens, B. Radiative impact of clouds on the shift of the Intertropical Convergence Zone. *Geophys. Res. Lett.* **41,** 4308–4315 (2014).

25. Grise, K. M. & Polvani, L. M. Southern Hemisphere cloud-dynamics biases in CMIP5 models and their implications for climate projections. *J. Clim.* **27,** 6074–6092 (2014).
26. Su, H. *et al.* Weakening and strengthening structures in the Hadley Circulation change under global warming and implications for cloud response and climate sensitivity. *J. Geophys. Res.* **119,** 5787–5805 (2014).
27. Wetherald, R. T. & Manabe, S. Cloud feedback processes in a general circulation model. *J. Atmos. Sci.* 1397–1416 (1988).
28. Mauritsen, T. *et al.* Climate feedback efficiency and synergy. *Clim. Dynam.* **41,** 2539–2554 (2013).
29. Kang, S. M., Held, I. M., Frierson, D. M. W. & Zhao, M. The response of the ITCZ to extratropical thermal forcing: Idealized slab-ocean experiments with a GCM. *J. Clim.* **21,** 3521–3532 (2008).
30. Voigt, A., Stevens, B., Bader, J. & Mauritsen, T. Compensation of hemispheric albedo asymmetries by shifts of the ITCZ and tropical clouds. *J. Clim.* **27,** 1029–1045 (2014).

Acknowledgements

A.V. and T.A.S. are supported by the David and Lucile Packard Foundation. T.A.S. is also supported by NSF award AGS-1255208. We thank L. Polvani for helpful comments, and H. Liu for downloading the CMIP5 aquaplanet data. We acknowledge the World Climate Research Programme's Working Group on Coupled Modelling, which is responsible for CMIP, and we thank the climate modelling groups of the Max Planck Institute for Meteorology and the Institute Pierre Simon Laplace for producing and making available their aquaControl and aqua4K aquaplanet simulations. For CMIP, the US Department of Energy's Program for Climate Model Diagnosis and Intercomparison provides coordinating support and led development of software infrastructure in partnership with the Global Organization for Earth System Science Portals.

Author contributions

A.V. designed the study and conducted the simulations. A.V. and T.A.S. analysed the data and wrote the manuscript.

Additional information

Supplementary information is available in the online version of the paper. Reprints and permissions information is available online at www.nature.com/reprints. Correspondence and requests for materials should be addressed to A.V.

Competing financial interests

The authors declare no competing financial interests.